Performance of the AGATA Gamma-ray Spectrometer in the PreSPEC Set-up at GSI

Lalovic, Natasa; Louchart, C.; Michelagnoli, C.; Perez-Vidal, R.M.; Ralet, D.; Gerl, J.; Rudolph, Dirk; Arici, T.; Bazzacco, D.; Clement, E.; Gadea, A.; Kojouharov, I.; Korichi, A.; Labiche, M.; Ljungvall, J.; Lopez-Martens, A.; Nyberg, J.; Pietralla, N.; Pietri, S.; Stezowski, O.; Collaboration, the AGATA; Collaboration, the PreSPEC

Published in:
Nuclear Instruments & Methods in Physics Research. Section A: Accelerators, Spectrometers, Detectors, and Associated Equipment

DOI:
10.1016/j.nima.2015.10.032

2016

Performance of the AGATA γ-ray Spectrometer in the PreSPEC Set-up at GSI

N. Lalović[a,b], C. Louchart[c], C. Michelagnoli[d], R. M. Perez-Vidal[e], D. Ralet[b,c], J. Gerl[b], D. Rudolph[a], T. Arici[f,b], D. Bazzacco[g], E. Clément[d], A. Gadea[e], I. Kojouharov[b], A. Korichi[h], M. Labiche[i], J. Ljungvall[h], A. Lopez-Martens[h], J. Nyberg[j], N. Pietralla[c], S. Pietri[b], O. Stezowski[k], and the PreSPEC and AGATA Collaborations

[a] *Department of Physics, Lund University, SE-22100 Lund, Sweden*
[b] *GSI Helmholtzzentrum für Schwerionenforschung GmbH, D-64291 Darmstadt, Germany*
[c] *Institut für Kernphysik, Technische Universität Darmstadt, D-64289 Darmstadt, Germany*
[d] *GANIL, CEA/DSM-CNRS/IN2P3, BP 55027, F-14076 Caen, France*
[e] *Instituto de Fisica Corpuscular, CSIC-Universitat de Valencia, E-46920 Valencia, Spain*
[f] *Justus-Liebig-Universität Giessen, D-35392 Giessen, Germany*
[g] *INFN Sezione di Padova and Dipartimento di Fisica, Università di Padova, IT-35131 Padova, Italy*
[h] *CSNSM, F-91405 Orsay Campus, France*
[i] *STFC Daresbury Laboratory, Daresbury, WA4 4AD Warrington, UK*
[j] *Department of Physics and Astronomy, Uppsala University, SE-75120 Uppsala, Sweden*
[k] *Université de Lyon, CNRS-IN2P3, Institut de Physique Nuclaire de Lyon, F-69622 Villeurbanne, France*

Abstract

In contemporary nuclear physics, the European Advanced GAmma Tracking Array (AGATA) represents a crucial detection system for cutting-edge nuclear structure studies. AGATA consists of highly segmented high-purity germanium crystals and uses the pulse-shape analysis technique to determine both the position and the energy of the γ-ray interaction points in the crystals. It is the tracking algorithms that deploy this information and enable insight into the sequence of interactions, providing information on the full or partial absorption of the γ ray. A series of dedicated performance measurements for an AGATA set-up comprising 21 crystals is described. This set-up was used within the recent PreSPEC-AGATA experimental campaign at the GSI Helmholtzzentrum für Schwerionenforschung. Using the radioactive sources ^{56}Co, ^{60}Co and ^{152}Eu, absolute and normalized efficiencies and the peak-to-total of the array were measured. These quantities are discussed using different data analysis procedures.

Email address: Natasa.Lalovic@nuclear.lu.se (N. Lalović)

The quality of the pulse-shape analysis and the tracking algorithm are evaluated. The agreement between the experimental data and the Geant4 simulations is also investigated.

Keywords: AGATA, gamma-ray spectroscopy, gamma-ray tracking, nuclear structure, pulse shape analysis, HPGe detectors

---

1. Introduction

Numerous exciting nuclear-structure phenomena can be probed by in-beam γ-ray spectroscopy experiments. Innovative approaches in design of dedicated detection systems during the past decades led to significant advances in position sensitivity, photopeak efficiency and peak-to-total ratio (P/T) in γ-ray spectroscopy. Moreover, the most recent γ-ray spectrometers, such as AGATA [1] and GRETA [2], brought about the new concept of high-resolution germanium tracking arrays. This paper starts out with a retrospective overview of large γ-ray arrays (Sec. 2) in order to introduce the developments and requirements of the new tracking arrays.

Here, the focus is the performance of AGATA in the framework of the recent PreSPEC-AGATA campaign at the GSI Helmholtzzentrum für Schwerionenforschung, Darmstadt, Germany [3, 4]. Incoming particle identification is done event by event by Fragment Separator (FRS) detector systems [5]. Details of the AGATA subarray configured for the PreSPEC-AGATA campaign are presented in Sec. 3.

Using Monte Carlo simulations based on the Geant4 toolkit [6], extensive characterization studies of AGATA were performed [7, 8]. Nevertheless, it is important for the feasibility and the success of the present and future experiments to check experimentally the validity and reliability of this simulation tool, as well as the calculated performance figures. Therefore, a dedicated source measurement was performed and is described in detail in Sec. 4. Furthermore, the quantities such as photopeak efficiency, normalized efficiency as a function of the γ-ray energy and P/T were investigated following the procedure outlined in

Sec. 5. The results of the analysis performed on the data alongside their interpretation and effect on other measurements are presented in Sec. 6. Moreover, these results were confronted to the output of the Geant4 simulation and their agreement is presented in Sec. 7.

Finally, the paper concludes with a short summary and an outlook for further investigations of performance of AGATA at GSI.

2. Concept of γ-ray Detection with AGATA

The strength of AGATA is the ability to obtain positions and deposited energies of individual γ-ray interactions. Applying γ-ray tracking makes it possible to determine the sequence of the interactions.

The sophisticated design of AGATA came about only after a series of advancements of large γ-ray detector arrays [9, 10]. At a very early stage of HPGe detectors' development, studies of nuclear structure could benefit from larger individual detectors, in comparison with Li-drifted Ge detectors. Further improvements focused on the increase of both the number of detectors and the solid angle covered by an array. This led to an enhancement of detection properties, mainly efficiency and energy resolution, and to some extent P/T. Additionally, a technique of background reduction was developed by means of Compton suppression. These efforts gave rise to the first arrays of HPGe detectors actively shielded by scintillating materials, which provided a substantial improvement of P/T.

Once a γ ray interacts with the detector medium, the energy recorded by those conventional arrays is the signal of any individual Ge-detector crystal. Typically, the absolute photopeak efficiency here depends on the intrinsic efficiency of the detector and its distance to the source. The P/T is determined by the intrinsic P/T of the individual detector elements, i.e. Ge detector plus surrounding Compton-suppression shield, and its geometry.

The next generation of Ge arrays relied on the novel idea of producing composite detectors, in particular the clover [11] and the cluster [12, 13] detectors.

Such detectors overcame the size limitation of the germanium crystals, while maintaining high granularity. This is important for the detection of long cascades of coincident γ rays. Arrays based on composite detectors increased efficiency over a large energy range and showed excellent P/T performance, thanks to the 'add back' concept [14], that uses signals from neighbouring Ge-detector crystals. Not only are the events originating in individual detectors summed to generate the total energy signal, but also the fraction of energies is recorded in cases of scattering between the crystals.

However, those detectors cover relatively large solid angles. This implies an uncertainty in γ-ray detection angle and quickly leads to Doppler-broadened peaks when studying γ-ray decays of fast-moving sources [15]. Secondly, it is difficult to distinguish two (or more) γ rays interacting at the same time in the same detector. This can lead to summing effects of coincident γ-ray transitions. The fact that those two γ rays are counted as one reduces the gain in efficiency and P/T provided by the advancement of composite detectors. Therefore, in the next generation of large γ-ray arrays the granularity was increased by means of additional contact segmentation [16, 17].

The innovative concept of segmentation ensured smaller opening angles of the individual granuli, which allowed for shorter detector-to-source distance, without deteriorating energy resolution due to Doppler broadening. As a consequence, the efficiency improved significantly [8]. The first arrays had longitudinal segmentation and made the localisation of the first interaction point in a two-dimensional plane possible [16, 17]. In this generation of detector arrays it was not the opening angle of the crystal as a unity that affected the Doppler broadening, but that of an individual segment instead. The above mentioned summing effects are also significantly reduced. Finally, the P/T of such detector arrangements can be enhanced.

The most recent developments followed the line of segmentation introduced above, and the idea of γ-ray tracking was realized through the three-dimensional segmentation (longitudinal and azimuthal) of HPGe crystals of specific tapered shape. The prerequisite to tracking are the determined interaction points provided by the pulse-shape analysis (PSA). As a consequence, Compton-suppression shields can be excluded. This allows to fill significantly more solid angle with Ge detectors. Currently two systems based on this principle are operational, one being in the U.S.A., GRETINA [2], and one in Europe, AGATA [1, 18–20].

The present work provides the feedback on the application of PSA algorithms and helps to evaluate the reconstruction quality with respect to all three coordinates, x, y and z.

There are two types of algorithms dealing with the tracking of the subsequent interactions of a γ-ray in a Ge crystal. The first one, which is called back-tracking [21, 22], is based on the reconstruction of the γ-ray path by starting the tracking procedure from the final interaction point. The second one is called forward-tracking [23–25] and starts by first recognizing clusters of interaction points. In this work, the forward-tracking algorithm is used and the results of the optimization are presented in Sec. 6.

3. AGATA Detector Configuration at GSI

In preparation for the HISPEC experiment at the FAIR-NuSTAR facility [26], the PreSPEC-AGATA campaign [3, 4] was conducted at GSI in 2012 and 2014. Here, secondary radioactive beams are produced by fission or fragmentation of a primary stable beam delivered by GSI accelerator complex and selected by the FRS [5]. These beams are directed to a secondary target at relativistic energies of several hundred MeV/u. The in-flight emitted γ rays coming from the secondary reactions are therefore affected by a significant Doppler shift: the sources are moving with velocities of about 50 % of the speed of light. The products of secondary nuclear reactions were discriminated using the Lund York Cologne CAlorimeter (LYCCA) [27].

The AGATA subarray, composed of 21 encapsulated detectors was placed at its nominal distance of 23.5 cm to the centre of the secondary target. Such a configuration ensured optimal energy resolution of Doppler-corrected γ-ray spectra, alongside the improved efficiency of the array compared with the earlier

RISING fast-beam set-up [15]. However, compared with the full AGATA array, this geometrical configuration results in only about 60 % of the crystal surfaces in contact with neighbouring ones. Thus the probability of γ rays escaping the active Ge volume is rather large, which limits the tracking performance compared to a full 4π tracking array.

According to the original design [1], AGATA consists of triple clusters of Ge crystals (cf. Fig. 1). Hosting AGATA at the final focal plane of the FRS required a modified arrangement. Because of the rather large beam-spot size, the most inner ring of five triple clusters needed to be replaced. Newly developed double clusters were then put in place to guarantee angular coverage at forward angles. This is due to the Lorentz boost, which has to be considered in case of γ rays emitted from nuclei moving at relativistic energies.

The arrangement of AGATA detectors in doubles and triples is shown in Fig. 1. The triples are enclosed by blue lines and the doubles by green lines. Dashed lines refer to missing crystals in two triple clusters, as well as one crystal from an AGATA double. Its electronics was used for the EUROBALL reference capsule (see Sec. 4).

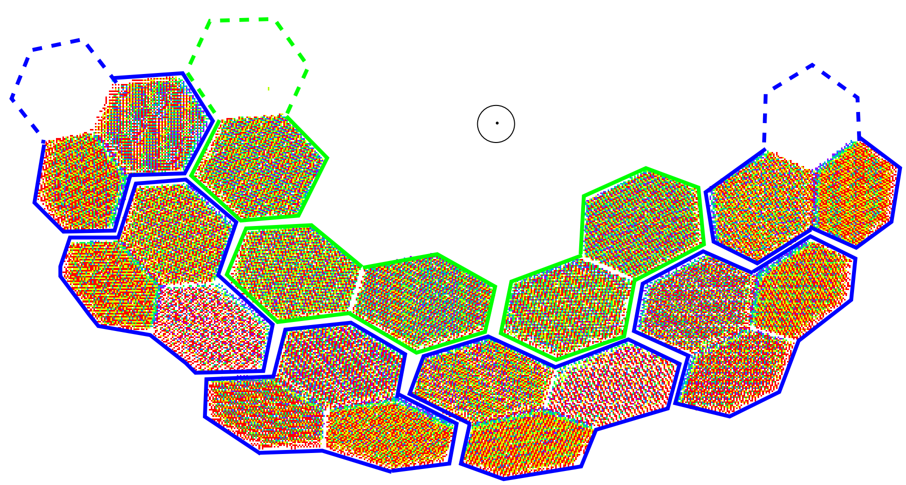

Figure 1: Configuration of AGATA at GSI during the PreSPEC-AGATA campaign. AGATA triples are enclosed by blue lines and AGATA doubles by green lines. Dashed lines indicate missing crystals. The $\odot$ symbol marks the beam direction.

4. Source Measurements

In order to analyze the in-beam experimental data, it is necessary to determine the response of the spectrometer by measuring efficiency and P/T. As mentioned before, simulations can be an excellent way to characterize, in a broad energy range, the performance figures for the campaigns employing AGATA. Nevertheless, simulated figures need to be checked thoroughly and, therefore, source measurements are required.

Early measurements at both LNL and GSI were severely hampered by factors such as the reduced number of encapsulated detectors present in the set-up, the uncertainties about the source position, the radiation background, the data acquisition dead time, to name but a few. Hence, a series of dedicated source measurements focusing on the determination of the absolute efficiency was performed within the scope of the PreSPEC-AGATA campaign at GSI in 2014.

The principal set-up comprised 21 36-fold segmented AGATA crystals positioned at the nominal target-array distance of 23.5 cm and one external non-segmented and electrically cooled detector [28], based on an EUROBALL capsule [12] as a reference (cf. Fig.2). It was intended to extract the absolute quantities, such as photopeak efficiency and P/T, in the most reliable manner. This was ensured by an approach, which is based on prompt coincidences of cascading γ rays between the external reference detector, i.e. the EUROBALL capsule, and all AGATA crystals.

Each of the AGATA crystals provides 38 signals: 36 for the segments and two for the core, namely two gains corresponding to a 5-MeV and a 30-MeV full range. The output of the respective preamplifier is digitized by means of a 100-MHz 14-bit ADC. This information is then sent via optical links to preprocessing cards, which perform the task of extracting the energy and time of a particular detector element [1]. To access the energy and time information, the Moving-Window Deconvolution (MWD) technique [29] and a leading-edge algorithm have been used, respectively. The outputs of this stage are transmitted to a computer farm performing further data processing, the overview of which is given in Ref. [30]. For more details on the complete data acquisition system employed in the PreSPEC-AGATA campaign, see Ref. [31].

For the source measurements, the electrically cooled EUROBALL capsule was integrated into the system in such a way that the signal from its preamplifier was sent to one of the AGATA digitizers. This ensured the same treatment of all crystals used for this measurement during data-taking. However, the fact that not all AGATA-tailored processing algorithms can be applied to or are relevant for the EUROBALL capsule led to further differentiation between these two detector types in the offline analysis. Data has been taken with standard

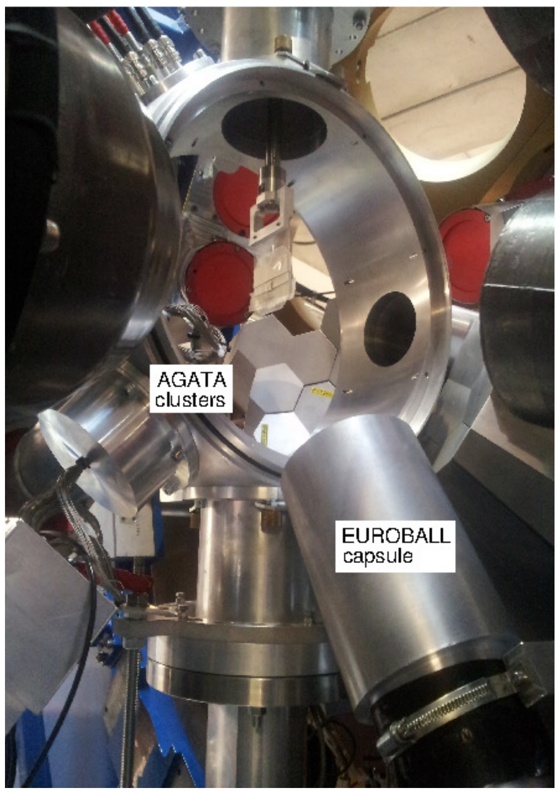

Figure 2: Part of the experimental set-up with the EUROBALL capsule, target station, and some AGATA clusters visible in the back. The EUROBALL capsule is located in the lower right corner.

γ-ray sources: ^{56}Co, ^{60}Co and ^{152}Eu. Each source was placed at the target position in the center of the PreSPEC-AGATA scattering chamber. During the in-beam experiments, this chamber holds the secondary target, so that the γ rays emitted from the target are to be detected by the surrounding array. For the measurements described here, the side parts of the scattering chamber were dismounted, whereas the holding ring structure was left in place. This can be seen in Fig. 2. The self-triggered data acquisition was handling the data generated by event rates up to 4 - 5 kHz per crystal.

In order to make a reliable efficiency estimate of direct use for the analysis of the stopped-beam experiments, the ^{60}Co and ^{152}Eu sources were also placed in front of and behind the plastic stopper. This 1 cm thick stopper was located 15 cm downstream from the focal point of the AGATA subarray. Then, averaging measurements of these two source positions, the efficiency values are extracted for the center of the plastic stopper. This position is denoted 'close position'. However, since these measurements were performed in between two in-beam experiments, additional material was present around the scattering chamber, namely its side parts and a 2 mm thick lead shielding. This has to be taken into account when interpreting particularly the low energy region of the spectra recorded under these conditions.

5. Analysis

5.1. Fine Tuning Prior to the Analysis

The processing of the signals from individual AGATA crystals and the essential calibration aspects are detailed in Ref. [30]. The processing takes place on two levels: on the *local* level all crystals are handled separately; on the *global* level the streams of processed data from individually treated crystals are assembled on the basis of time-stamp and processed further as events. The sequence of processing stages and a schematic overview are outlined in Appendix A.

In order to derive the interaction positions a number of tests with several PSA algorithms was performed. Although different, those algorithms had no apparent effect on the results and the analysis was conducted with the standard

PSA algorithm, Adaptive Grid Search [33], considering single interaction in a segment.

Since the EUROBALL capsule was integrated as if it were one of the AGATA crystals, its data was processed in the same way as an AGATA crystal.

In this measurement events were constructed using all the data from the crystals within a time window of 100 ns. Thereafter, the tracking algorithm was applied on the AGATA data exclusively, which is discussed thoroughly in Sec. 5.2.

5.2. Absolute Efficiency and Peak-to-Total

One of the main tasks of the data analysis was to determine the absolute efficiency of the AGATA array, depending on data treatment and parametrization. Thereby, two different approaches have been employed. The data taken with a ^{60}Co source utilizes its cascade of two coincident γ rays at 1332 and 1173 keV. In the first approach, the so-called *external trigger method*, the coincidences between AGATA crystals and the EUROBALL capsule as a reference are studied. The second approach is the *sum-peak method*, focusing on AGATA crystals only where no coincidences were used. In the external trigger method, a $\gamma\gamma$ angular correlation correction of 0.981(5) is applied for the ^{60}Co cascade, corresponding to the average angle between the AGATA crystals and the EUROBALL capsule.

5.2.1. External Trigger Method

Events which fulfilled the trigger requirement from the reference detector within a 100 ns time window were selected for this approach. The energy spectra representative for the whole array were created, depending on the modes in which AGATA can be operated at the data-analysis stage:

- core common: takes into account individual energies registered by the central contacts;
- calorimetric: total sum of energies recorded by all central contacts of all AGATA crystals;

- tracked: uses the reconstructed energy, which is subject to the tracking performance and thus choice of tracking parameters.

- tracked, excluding single interaction: same as the previous mode except that it discards events with only a single interaction point up to the energy of 800 keV.

- add-back: selectively sums single hits in an event found within a sphere of 100 mm radius. The reference point for this approach was the hit with maximum energy deposition.

The absolute efficiency at 1173 keV in all five analysis modes is extracted from the ratio of the intensity in the 1173 keV peak measured by AGATA crystals over the intensity of the 1332 keV peak measured by the EUROBALL capsule. In this case, P/T was calculated as a ratio of the yield of the peak at 1173 keV and the total number of counts in the spectrum.

Furthermore, in case of the tracking mode of analysis, the impact of the AGATA tracking algorithms on the performance was studied. This is explained in more detail in Sec. 6.3.

5.2.2. Sum-Peak Method

In this approach, the absolute efficiency was determined using the sum-peak method [34, 35]. Data collected by the reference detector was not used in this case. AGATA was treated as a calorimeter, resulting in a total spectrum where the energies from all central contacts have been summed up. Thus, the absolute efficiency at 1173 keV was measured from the ratio of the intensity in the sum-peak at 2505 keV over the intensity of the 1332 keV peak. In this case, P/T was calculated as a ratio of the sum of the ^{60}Co peaks intensities and the total counts in the spectra up to 1350 keV. For a reliable efficiency estimate, a correction for random coincidences was performed, quantifying it from the activity of the source used in the measurement. Additionally, rare cases of multiple cascades have also been accounted for.

The use of the external trigger method was motivated in Sec. 4 as the most reliable method to extract the absolute efficiency, hence the thorough consideration of different analysis modes. In contrast, for the sum-peak method only the calorimetric mode of analysis was used to simply cross check the values obtained with the external trigger method.

5.3. Normalized Efficiency

Data taken with the ^{56}Co and ^{152}Eu sources provide the energy dependence of the efficiency in the γ-ray energy range from 120 to 3300 keV. To combine the two data sets collected with the two aforementioned sources separately, the spectrum of the former was normalized with respect to the 867-keV line of the latter, since the ^{56}Co source emits a γ ray of similar energy, namely 847 keV. For this method, calorimetric, core common and the tracked mode of analysis were used.

Data taken with the ^{152}Eu source alone has also been analyzed by means of the add-back routine. To normalize the yields obtained in this way, the absolute efficiency from the external trigger method was utilized (see Sec. 5.2.1). Furthermore, performance of the tracking has been tested on the data taken with the ^{152}Eu source only (see Sec. 6.3).

In order to obtain the normalized efficiency curve for the stopped-beam data from the PreSPEC-AGATA campaign, data collected with the ^{152}Eu source at the so-called 'close position' (see Sec. 4) has been analyzed. Thereby, the energy information from the central contact of all crystals was employed. Finally, the yields of standard γ lines recorded at two different positions were averaged and normalized to the absolute efficiency.

6. Results

6.1. Absolute Efficiency and Peak-to-Total

The values obtained for the absolute efficiency and P/T values at 1173 keV are shown in Table 1.

Table 1: Efficiency and P/T at 1173 keV obtained for different modes of data treatment. The statistical uncertainties are indicated in parenthesis. Tracking refers to default parameters (cf. Sec. 6.3). See text for details.

Input	Efficiency (%)	P/T (%)
AGATA (external trigger method)		
Core Common	2.38(2)	18.3(2)
Calorimetric	3.30(2)	32.2(3)
Tracked with single interactions	2.55(3)	37.5(4)
Tracked without single interactions	2.53(3)	42.3(5)
Add-back 100 mm	2.86(4)	24.6(2)
Geant4 simulations (external trigger method)		
Core Common	2.84(9)	22.5(6)
Calorimetric	4.21(8)	42.5(10)
Tracked with single interactions	2.53(8)	58.2(19)
AGATA only		
Sum-peak calorimetric	3.25(4)	30.0(5)

As seen in the table, the values derived for the absolute efficiency, ϵ, differ significantly for the various modes of extracting the energies from the AGATA detectors. In the conventional approach, the efficiency was determined only taking into account energy information from the central contact of each single crystal. This core-common treatment results in the lowest value of $\epsilon = 2.38(2)$ % and the poorest $P/T = 18.3(2)$ %. Since AGATA has no Compton-supression shields, about 60 % of the Compton-scattered events escaping the crystals will increase the background of the spectra by producing counts in both neighbouring crystals. Therefore, such low value of the P/T is understood. A pronounced increase in both efficiency and P/T is observed when referring to AGATA as a calorimeter, namely $\epsilon = 3.30(2)$ % and $P/T = 32.2(3)$ %, respectively. The calorimetric mode takes into account not only full-absorption in a crystal, but also Compton-scattering into neighbouring crystals. Therefore, more events are registered in the full-energy peak, simply because energy portions, which the core-common mode predominantly interprets as background, are summed up. In general, the calorimetric mode is sensitive to summing up multiple γ rays, particularly in case of high-fold cascading γ rays.

In order to apply tracking algorithms on the present data sets, an adjustment in the data processing was implemented. The absolute efficiency measurement relies on coincidences between AGATA and the reference EUROBALL capsule, but only AGATA crystals are included in the tracking routine. Therefore, two classes of detectors have been defined in the analysis procedure: one for the EUROBALL capsule alone and the other one for all AGATA crystals, which registered a signal in a coincident event. This allowed for a separate treatment of different detectors taking part in coincident events, yet being implemented in the same DAQ system. Finally, this approach led to an efficiency of $\epsilon = 2.55(3)$ % and $P/T = 37.5(4)$ %. The efficiency is obviously lower than the one in calorimetric mode of analysis, but P/T shows a significant improvement.

The results of the calorimetric mode suggest that summing up all energies recorded by all crystals could enhance lower-energy contributions, leading to somewhat deteriorated P/T. Additionally, this approach does not allow for rejection of partially absorbed γ rays and, as stated in Sec. 3, around 40 % of the detector surface is not covered by other neighbouring detectors. Therefore, all partially absorbed γ rays are included in the calorimetric spectrum.

As compared to the calorimetric mode, the tracked mode results in better P/T. Tracking relies on properly extracted sequences of γ-ray energies and points and rejection of the γ rays that could not be reconstructed. Hence, it replaces the Compton suppression shields to some extent. If performed successfully, it suffers less from background contributions.

As explained in Sec. 5.2, the single-interaction contributions, being clusters with single hits in a detector, could be excluded from the spectrum obtained after tracking. This modification yields an efficiency of $\epsilon = 2.53(3)$ % and $P/T = 42.3(5)$ %. The single interactions are largely responsible for the low-energy part of the spectrum, hence the better P/T values as seen in Tab. 1. Fig. 3 depicts this property of the spectra obtained with and without single interactions. Due to a hard-coded limit, the spectral response of single interactions extends up to 800 keV. Recent work [36] suggests that those events account for ~ 20 % of the photopeak yield at 1173 keV. Therefore, the efficiency value reported here might show a corresponding increase if setting the energy acceptance limit for the single interactions as high as the γ rays of ^{60}Co.

The sum-peak method (see Sec. 5.2.2) yields results similar to the calorimetric mode, namely $\epsilon = 3.25(4)$ % and $P/T = 30.0(5)$ %.

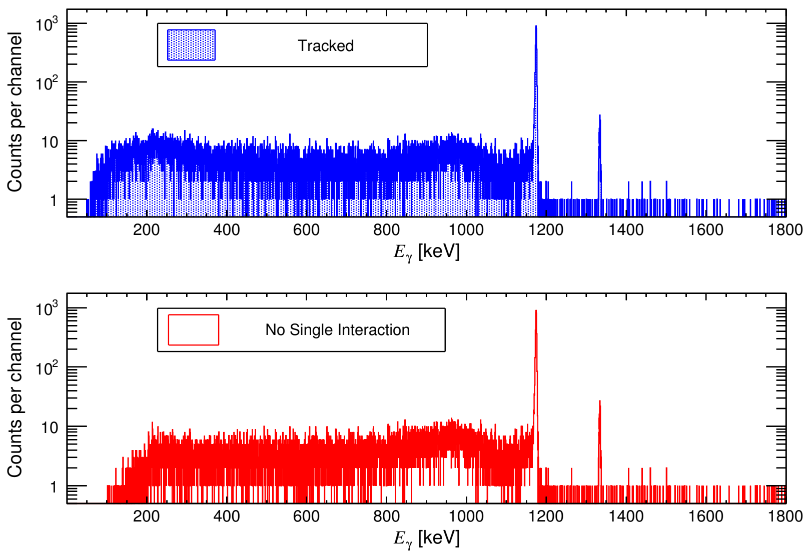

Figure 3: Spectra obtained with the MGT tracking algorithm [24] including (upper panel) and excluding single interaction points up to 800 keV (lower panel).

6.2. Normalized Efficiency

Different in-beam experiments performed with AGATA at GSI focused on different γ-ray energy regions. Therefore, a reliable reference in terms of an energy-dependent efficiency curve is needed. In this work, the energy extends up to $\sim$ 3.3 MeV, i.e. one of the γ-ray transitions originating from the ^{56}Co source measurement. Three modes of operating AGATA at the data-analysis stage have been considered for the combined data set of ^{56}Co and ^{152}Eu: core common, calorimetric, and tracked with default parameter values (*Figure of Merit* FOM = 10, see Sec. 6.3). For the analysis of the three respective cases, two spectra-analysis programs were used: tv [37] and TkT [38]. All γ-ray lines were least-squares fitted several times with a convolution of a Gaussian, a function that accounts for eventual tails on either right or left side of the centroid and another set of functions used to estimate the background. These fit results, including systematic uncertainties, were then sent to the code EFFIT, included in the Radware software package, which is using the parametrization detailed in [39] to extract the efficiency values from the measured peak intensities. The function used to fit the data points from the ^{56}Co and ^{152}Eu data sets is [39]:

$$\ln \epsilon(E_\gamma) = \{(A + B * x + C * x^2)^{-G} + (D + E * y + F * y^2)^{-G}\}^{-1/G} \tag{1}$$

with $x = \ln(E_\gamma/100)$, $y = \ln(E_\gamma/1000)$, E_γ in units of keV and A, B, C, D, E, F, G as fit parameters. Provided the absolute values of efficiency at 1173 keV (see Sec. 6.1 and Table 1), the aforementioned efficiencies can be readily normalized to the absolute efficiencies of the respective mode:

$$\epsilon_{\text{abs}}(E_\gamma) = N \cdot \epsilon(E_\gamma) \tag{2}$$

The efficiency curves according to Eq. 1 for different modes of analysis, alongside the experimental values for the calibration sources, are shown in Figs. 4, 5 and 7. The values of the fit and normalization parameters for all the curves are listed in Table 2.

Table 2: Fit parameters using the program EFFIT [39]. In all cases the parameters $C = 0$ and $G = 12$ were kept fixed. See text for details.

		Parameters					
Dataset	Mode	A	B	D	E	F	N
^{152}Eu and ^{56}Co	Core Common	8.42(19)	2.66(21)	6.410(3)	-0.573(6)	-0.071(6)	0.00454(3)
	Calorimetric	7.43(4)	1.69(5)	6.579(2)	-0.391(5)	–	0.00513(3)
	Tracked	6.80(5)	5.60(11)	6.3882(25)	-0.452(5)	–	0.00478(4)
^{152}Eu	Tracked FOM = 1.0	6.89(6)	5.73(12)	6.374(3)	-0.438(5)	–	0.00460(4)
	Tracked FOM = 0.1	7.7(3)	6.7(4)	6.274(4)	-0.421(6)	–	0.00440(5)
^{152}Eu	Add-back 100 mm	7.77(5)	1.86(6)	6.5653(24)	-0.413(5)	–	0.00423(5)
	Close Position	3.11(7)	2.9(3)	4.375(5)	-0.377(20)	-0.272(20)	0.038(2)

In case of the calorimetric spectrum, it is obvious that certain data points lie somewhat away from the least-squares fit (green stars in Fig. 4). Comparison of the γ-ray spectra has shown enhanced yields or slight modification in peak shapes. These differences in the shape of the peak in the calorimetric spectrum can arise from another process resulting in very similar energy deposition, i.e. summing of either two coincident γ rays or a γ ray and an X ray.

The drop in tracking efficiency below 100 keV is in part related to the approximation made to compute effective distances in Ge. The approximation of a Ge sphere leads to an overestimation of the distance traveled by photons into the detector by up to a few mm. This overestimation is extremely penalizing for low-energy photons, which have very small ranges in Ge and are therefore awarded a poor figure of merit.

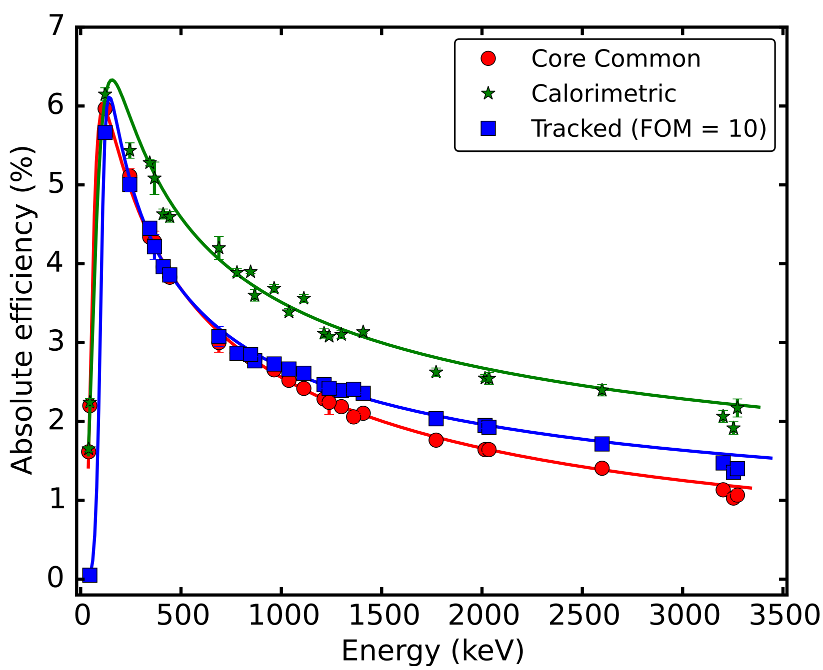

Figure 4: Efficiency curves obtained with spectra collected with ^{56}Co and ^{152}Eu normalized to the absolute efficiency determined at 1173 keV and confirmed by an external trigger method with the ^{152}Eu source data.

The results with the ^{152}Eu source at 'close position' (cf. Sec. 4) as well as the add-back treatment in case of the nominal position of the source are shown in Fig. 5. The two mentioned curves are compared to the core-common efficiency derived from the data collected with the same source at nominal position. In case of the core common at the close position the low-energy part of the spectrum is strongly affected by the lead shielding around the scattering chamber. Another cause of the attenuated yields is that this curve was derived by placing the ^{152}Eu source both in front and behind the plastic stopper. Consequently, in the first case the γ rays had to travel through the plastic medium, which reduced the low-energy contributions. In contrast to low energies, in the region of $E_\gamma \gtrsim 500$ keV the enhancement in the efficiency is ensured by the vicinity of the source.

6.3. Influence of the tracking algorithms

Two codes based on the forward-tracking algorithm mentioned in Sec. 2, both used by the AGATA community, have been employed to further investigate the effect of tracking on the performance. The details of the OFT performance are discussed in Ref. [36], whereas this work focuses on the MGT performance. The details of its implementation are, however, not subject of this work. They can be found in Ref. [24].

MGT and OFT tracking algorithms start by grouping certain interaction points which may be a part of the same physical event, resulting in one *track*. These groups of candidates are called *clusters*. The interaction points in each cluster are thus accepted in a given sequence or eventually rejected based on the conditions demanded by the algorithm.

In general, for the so-called FOM only one MGT parameter is varied, which defines how restrictive the algorithm is to the data sent as an input [24]. It quantifies divergence from the accepted χ^2 value, which is calculated between the ideal angle-energy sequence and the measured one. The higher the FOM value, the more data satisfy the MGT criteria, because the clusters are evaluated with greater 'tolerance', and vice versa. Consequently, for very high values of

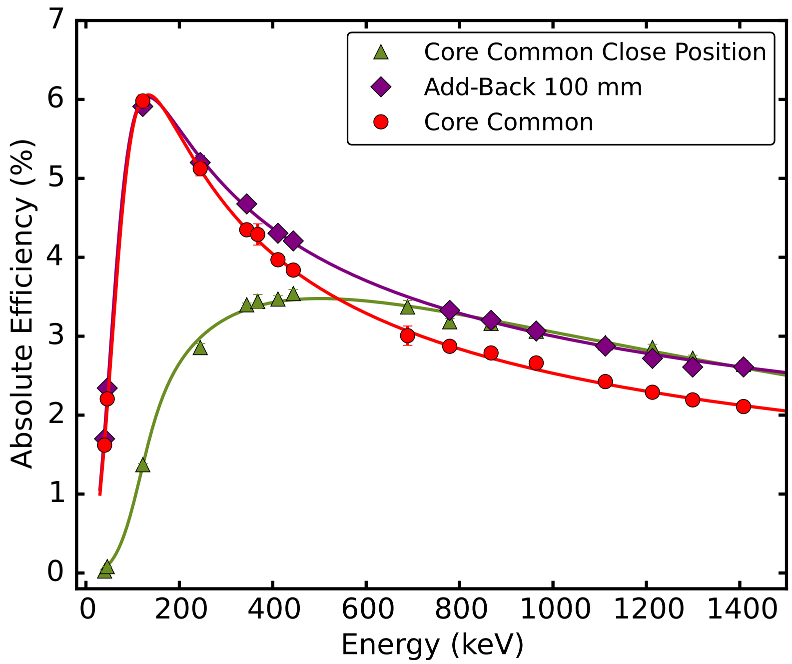

Figure 5: Efficiency curves obtained with spectra collected with ^{152}Eu normalized to the absolute efficiency determined at 1173 keV. The green curve (triangle up) and the red curve (circle) both represent the results when utilizing core common energy information but at two different positions: the green curve being closer to the array and the red at the nominal position. The purple curve (diamond) is obtained after adding back all hits in an event, which occurred within 100 mm radius from the reference point (highest energy release).

the FOM, more data has been interpreted as 'good'. But it also happens that the algorithm considers more events as background or it simply, due to the possible surplus of lower-energy contributions, does not classify the events in clusters well enough as a part of a real Compton scattering sequence.

The behaviour of tracking efficiency and P/T with respect to the absolute tracking efficiency has been tested in MGT [24] and OFT [25, 36], respectively. This was done by 'tuning' the FOM by changing the tracking parameters which are left free for the user to modify.

The effect of changing the FOM can be seen in Fig. 6. The curves show

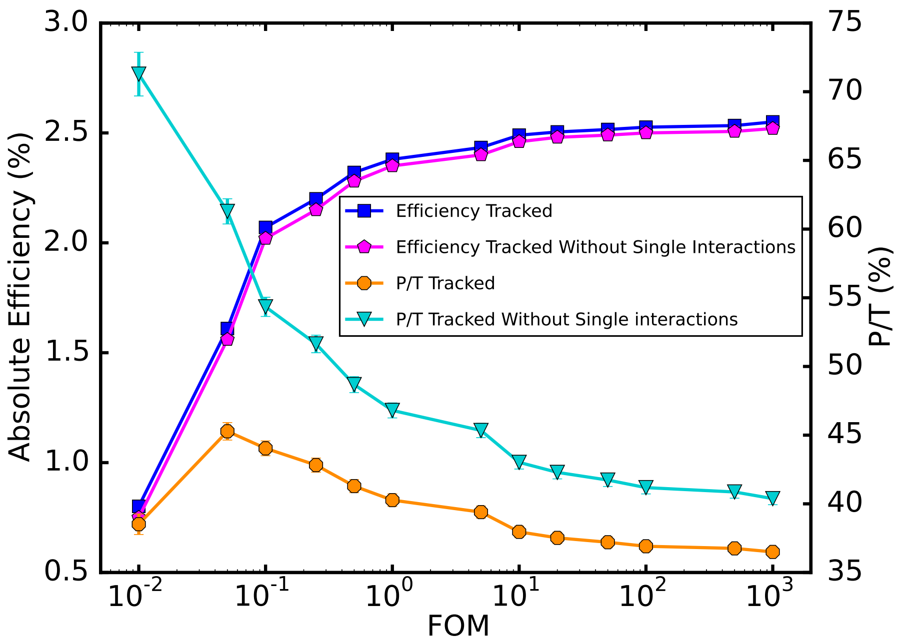

Figure 6: Influence of the FOM on the efficiency and P/T. FOM values range from 0.01 (left) to 1000 (right). All curves are obtained after applying the MGT tracking algorithm on ^{60}Co data. The blue curve (squares) represents the tracked efficiency trend for varying FOM. The magenta curve (pentagons) is a result of the same procedure, only without single interactions being treated. The orange curve (octagon) shows how the tracked P/T is affected by different values of the FOM. Similarly, the turquoise curve (triangle down) shows the behaviour of the same quantity, only referring to the tracked data without single interactions.

how the efficiency at 1173 keV and P/T change as the FOM varies. The efficiency is increasing with higher FOM, unlike the P/T. For higher values of the FOM, more events have fulfilled the requirement of the algorithm. Hence, one can expect enhancement in the intensity of the full-energy peak, thus in the absolute efficiency. This increase comes about at the cost of deteriorated P/T. However, after subtracting single-interaction contributions in the tracked spectra (see Sec. 6.1), a significant enhancement in the P/T is obtained (see Fig. 6). In the range of the tested FOM values the absolute efficiency exhibits an increasing trend for the lower values of the FOM. This behaviour is less pronounced for the rest of the range, as the absolute efficiency could not raise infinitely. Additionally, the further decrease of the P/T and the interplay of the two quantities suggest that the overall sensitivity of the system might not continue to improve significantly as the FOM increases. Therefore, the optimum value of the FOM should be decided by the user, in such a way to benefit from the changes in the values of the absolute efficiency and P/T. The MGT default value is set to FOM = 10 [24].

Moreover, consideration of the optimum FOM value is essential when applying tracking algorithms to different in-beam data sets. Beside Fig. 6, which shows that there is practically no increase in efficiency for FOM $\gtrsim$ 10, there are several criteria to be considered. Firstly, how the value of the FOM might affect the results in an energy region of interest for a certain experiment. Secondly, if choosing the tracked spectrum with or without single interactions could serve as a reference alone, again depending on the energy region of interest. Finally, the selection of the best FOM might also depend on γ-ray multiplicity.

Additionally, the analysis of the ^{152}Eu data after tracking provides decisive input for treatment of the in-beam data. This implies the consideration of the ^{152}Eu dataset in the tracked mode alone, whilst varying the FOM. As in Section 6.2, the measured values of efficiency were normalized with respect to the absolute efficiency for different values of FOM and the fitting routine [39] generated the corresponding curves. Figure 7 shows that the general trend of the efficiency curve is independent of the variation in FOM. Instead, only the absolute value of efficiency is affected by changes of the FOM. As in case of ^{60}Co data, efficiency increases as the FOM increases. Following the analysis with different values of the FOM (see Fig. 6), the three values of the FOM were selected and displayed in Fig. 7, since further increase of the FOM does not affect the values of absolute efficiency significantly. This property is, as expected, in accordance with the analysis performed on the ^{60}Co data, which strengthens the argument of choosing the appropriate FOM value.

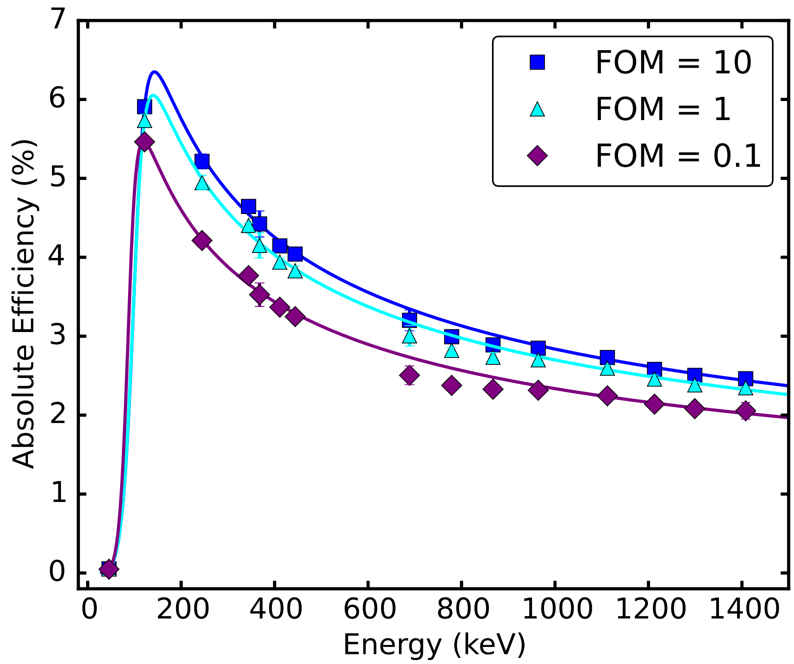

Figure 7: Efficiency curves obtained with a ^{152}Eu source by varying the FOM in the MGT tracking algorithm.

7. Geant4 Simulations

The developed Geant4 simulation comprises a realistic implementation of the set-up used during the source measurement including the scattering station with the holding ring structure as seen in Fig. 8. The evaluated results suggest the absolute efficiency for the core-common treatment of $\epsilon = 2.84(9)$ % and $P/T = 22.5(6)\%$, $\epsilon = 4.21(8)$ % and $P/T = 42.5(10)$ % for operating AGATA in calorimetric mode and $\epsilon = 2.53(8)$ % and $P/T = 58.2(19)\%$ for the tracking approach. The results from the simulation are somewhat higher than the experimental ones (see Table 1). They are also free from random coincidences. To first order, this can be associated to the difference between ideal detectors in the simulation and real detectors used for the experimental campaign at GSI. Despite these small discrepancies, detailed Geant4 simulations are a valuable tool in optimizing the tracking parameters for (in-beam) data analysis.

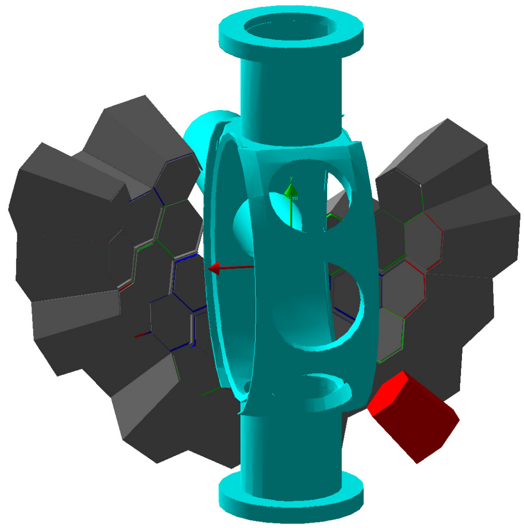

Figure 8: Geant4 visualization of the set-up. All AGATA crystals placed around the scattering chamber and the holding structure and the EUROBALL capsule are depicted solid. When used in the full PreSPEC-AGATA set-up, the beam enters from the front side. The EUROBALL capsule, shown in red, is located in the lower right corner.

8. Summary

The performance of the AGATA subarray at GSI has been presented, with the main figures absolute efficiency and P/T being evaluated. Twenty one AGATA crystals were employed in the experimental campaign at GSI, after which the characterization measurements using calibration sources were performed. Several practical aspects of applying the tracking algorithms on the source data have been described, as well as some issues which need to be considered in case of in-beam data taken during the PreSPEC-AGATA campaign at GSI. Additionally, the same data has been analyzed by exploiting only the energy recorded by the central contact of all crystals, in the so-called core-common mode, as well as summing up energies recorded by all crystals, in the calorimetric mode. The measured values of the absolute efficiency do vary, but they do so in a predictable manner, as shown by the calorimetric efficiency being larger than the core-common. This consideration affects the in-beam data in such a way that the optimal treatment should be found for each experiment individually.

Moreover, further studies should focus on high γ multiplicity effects by both adding events recorded during measurements with sources and in in-beam events. This aspect should help understand the properties of γ-ray spectra taken in in-beam conditions.

Acknowledgements

This work has been supported by the European Community FP7-Capacities, contract ENSAR No. 262010 and by the Swedish Research Council and the Knut and Alice Wallenberg Foundation. This work has also been supported by the BMBF under Nos. 05P09RDFN4, 05P12RDFN8, by the LOEWE center HIC for FAIR, and by the UK Science and Facilities Research Council. AG and RMPV were partially supported by MINECO, Spain, under the grants FPA2011-29854-C04, FPA2014-57196-C5, Generalitat Valenciana, Spain, under the grant PROMETEOII/2014/019 and EU under the FEDER program.

Appendix A. Overview of Data Processing

All the operations on the data are performed with dedicated Narval [32] chains - the so-called actors on the data - implemented via C++ classes.

The data from the EUROBALL capsule was processed in the same way as from an AGATA crystal but with one exception, namely the *Tracking* actor. Furthermore, the EUROBALL capsule is a single non-segmented HPGe detector and the PSA was only formally performed on it. In practice, the algorithm

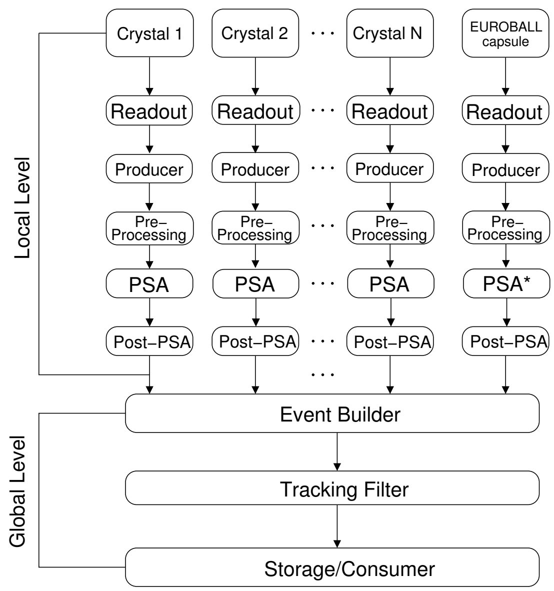

Figure A.1: Structure of AGATA Data Processing; here $N = 21$. Each box corresponds to a Narval actor. The EUROBALL capsule is also integrated in the system. The PSA associated to it was marked with an asterisk due to the fact that it was applied only formally. See text for details.

applied to it differs significantly from the sophisticated AGATA-tailored algorithms. Basically, every interaction is treated as if it had happened in the center of the crystal.

[1] S. Akkoyun *et al.*, Nuclear Instruments and Methods in Physics Research Section A 668 (2012).

[2] M.A. Delaplanque *et al.*, Nuclear Instruments and Methods in Physics Research Section A 430 (1999) 292.

[3] N. Pietralla *et al.*, Eur. Phys. J. Web of Conferences 66 (2014) 02083.

[4] P. Boutachkov *et al.*, to be published.

[5] H. Geissel *et al.*, Nuclear Instruments and Methods in Physics Research Section B 70 (1992) 286.

[6] S. Agostinelli *et al.*, Nuclear Instruments and Methods in Physics Research Section A 506 (2003) 250.

[7] E. Farnea *et al.*, Nuclear Instruments and Methods in Physics Research Section A 621 (2010) 331.

[8] C. Domingo-Pardo *et al.*, Nuclear Instruments and Methods in Physics Research Section A 694 (2012) 297.

[9] C.W. Beausang and J. Simpson, Journal of Physics G: Nuclear and Particle Physics 22 (1996) 527.

[10] J. Eberth and J. Simpson, Progress in Particle and Nuclear Physics 60 (2008) 283.

[11] F.A. Beck, Proceedings of the Conference on Physics from Large γ-ray Detector Arrays, Berkeley, LBL 35687, CONF 940888, UC 413 (1994) 154.

[12] J. Eberth, Progress in Particle and Nuclear Physics 28 (1992) 495.

[13] J. Eberth *et al.*, Nuclear Instruments and Methods in Physics Research Section A 369 (1996) 139.

[14] G. Duchêne *et al.*, Nuclear Instruments and Methods in Physics Research Section A 432 (1999) 90.

[15] H.J. Wollersheim *et al.*, Nuclear Instruments and Methods in Physics Research Section A 573 (2005) 637.

[16] J. Simpson *et al.*, Acta Physica Hungarica 11 (2000) 159.

[17] D. Habs *et al.*, Progress in Particle and Nuclear Physics, 38 (1997) 1.

[18] J. Gerl, Acta Physica Polonica B 34 (2003) 2481.

[19] J. Simpson, Journal of Physics: Conference Series 41 (2006) 72.

[20] A. Gadea *et al.*, Nuclear Instruments and Methods in Physics Research Section A 654 (2011) 654.

[21] J. Van der Marel and B. Cederwall, Nuclear Instruments and Methods in Physics Research Section A 477 (2002) 391.

[22] L. Milechina and B. Cederwall, Nuclear Instruments and Methods in Physics Research Section A 508 (2003) 394.

[23] G.J. Schmid *et al.*, Nuclear Instruments and Methods in Physics Research Section A 430 (1999) 69.

[24] D. Bazzacco, MGT code developed within the TMR program "Gamma-ray tracking detectors", Nuclear Physics A 746 (2004) 248c.

[25] A.Lopez-Martens *et al.*, Nuclear Instruments and Methods in Physics Research Section A 533 (2004) 454.

[26] A.M. Bruce *et al.*, to be published.

[27] P. Golubev *et al.*, Nuclear Instruments and Methods in Physics Research Section A 723 (2013) 55.

[28] I. Kojouharov, H.-J. Wollersheim, J. Gerl, M. Wolf, T. Engert. GSI Scientific Report 2008, GSI Report 2009-1 (2009) 235.

[29] A. Georgiev *et al.*, IEEE Transactions on Nuclear Science 41 (1994) 1116.

[30] N. Lalović *et al.*, Eur. Phys. J. Web of Conferences 93 (2015) 07007.

[31] D. Ralet *et al.*, Nuclear Instruments and Methods in Physics Research Section A 786 (2015) 32.

[32] X. Grave *et al.*, Real Time Conference 14th IEEE-NPSS (2005) 5.

[33] R. Venturelli and D. Bazzacco, LNL Annual Report 2004, (2004) 220.

[34] I. Kim, C. Park and H. Choi, Applied Radiation and Isotopes, 58 (2005) 199.

[35] J. M. R. Hutchinson, W. B. Mann and P. A. Mullen, Nuclear Instruments and Methods 112 (1973) 187.

[36] A.Lopez-Martens *et al.*, submitted to Nuclear Instruments and Methods in Physics Research Section A.

[37] J. Theuerkauf, S. Esser, S. Krink, M. Luig, N. Nicolay, O. Stuch, and H. Wolters, program TV, University of Cologne, unpublished.

[38] D. Bazzacco, The TkT spectrum viewer, private communication.

[39] D.C. Radford, Nuclear Instruments and Methods in Physics Research Section A 361 (1995) 297.